

## Structure of $^{15,16}\text{C}$ and phenomenology of the hindered $E2$ transition in $^{16}\text{C}$

Y. Suzuki,<sup>1</sup> H. Matsumura,<sup>2</sup> and B. Abu-Ibrahim<sup>1,3</sup>

<sup>1</sup>*Department of Physics, Niigata University, Niigata 950-2181, Japan*

<sup>2</sup>*Graduate School of Science and Technology, Niigata University, Niigata 950-2181, Japan*

<sup>3</sup>*Department of Physics, Cairo University, Giza 12613, Egypt*

(Received 15 July 2004; published 18 November 2004)

The three-body model of  $^{14}\text{C}+n+n$  is applied to study the  $E2$  transition in  $^{16}\text{C}$ . The  $n$ - $^{14}\text{C}$  potential is chosen to reproduce the single-particle energies of  $^{15}\text{C}$ . The wave functions of  $^{16}\text{C}$  are obtained as a combination of correlated Gaussians by including the Pauli requirement. It is found that the hindered  $E2$  transition can be accounted for by a polarization charge of about  $0.10e$  while the  $E2$  transition in  $^{15}\text{C}$  requires a little larger charge of  $0.16e$ . The soundness of this result is contrasted to the  $E2$  transitions in ( $^{17}\text{O}$ ,  $^{18}\text{O}$ ) and ( $^{17}\text{F}$ ,  $^{18}\text{Ne}$ ) nuclei. The longitudinal momentum distribution of  $^{15}\text{C}$  fragments from  $^{16}\text{C}$  breakup can be well reproduced.

DOI: 10.1103/PhysRevC.70.051302

PACS number(s): 27.20.+n, 21.60.-n, 23.20.Js, 25.60.Gc

Electric quadrupole ( $E2$ ) transitions provide us with important information on the deformation of transition charge density. The enhancement of  $E2$  transition probabilities suggests that more active nucleons contribute to the transition, thereby pointing to a kind of collectivity beyond a single-particle motion. Measurements of  $E2$  transition strength for exotic nuclei are in progress and give us information on a new region of deformation [1,2] or the vanishing of magic numbers which reflect the stability of the nuclear mean field. Very recently the  $E2$  transition from the first  $2^+$  state to the ground  $0^+$  state in  $^{16}\text{C}$  has been studied through a lifetime measurement using a recoil shadow method [3] and  $^{16}\text{C}+^{208}\text{Pb}$  inelastic scattering [4]. The  $B(E2)$  value is found to be  $0.63 \pm 0.12 e^2 \text{fm}^4$ , which corresponds to anomalously small strength of about 0.26 W.u. The anomaly is apparent by a comparison between  $^{14}\text{C}$  and  $^{16}\text{C}$ .  $^{14}\text{C}$  is neutron closed and  $^{16}\text{C}$  has two more neutrons, so the energy of the first excited state is expected to be lower in  $^{16}\text{C}$  than in  $^{14}\text{C}$ . In fact the excitation energy is 1.77 MeV for  $^{16}\text{C}$  whereas it is 7.01 MeV for  $^{14}\text{C}$ . Therefore the  $B(E2)$  value of  $^{16}\text{C}$  is expected to be larger than that of  $^{14}\text{C}$ . In spite of this expectation the  $B(E2)$  value of  $^{16}\text{C}$  is much smaller than that of  $^{14}\text{C}$ , which is  $3.74 e^2 \text{fm}^4$  (1.87 W.u.).

The purpose of this investigation is to study the structure of  $^{16}\text{C}$  by focusing on a mechanism which leads to the hindered transition in  $^{16}\text{C}$ . Our basic assumption is that the relevant levels of  $^{16}\text{C}$  are generated from a  $^{14}\text{C}+2n$  model. We consider the structure of  $^{15}\text{C}$  as well in a  $^{14}\text{C}+n$  model. There are some evidences which support the model. First  $^{14}\text{C}$  can practically be considered inert as equally well as  $^{16}\text{O}$  because the excitation energy of the first excited state is fairly high (about 6 MeV) in both nuclei. Secondly the data on fragmentation experiment are available [5–7] and in particular the momentum distribution of  $^{14}\text{C}$  fragment from the breakup of  $^{15}\text{C}$  confirms the one-neutron halo structure of  $^{15}\text{C}$  [5]. Thirdly spectroscopic information on particle-hole configurations in  $^{16}\text{C}$  has recently been extended to high excitation energy [8]. The  $^{14}\text{C}(t,p)$  reaction in particular supports the  $^{14}\text{C}+(sd)^2$  configuration for the ground and first excited states of  $^{16}\text{C}$  [9]. Fourthly the inelastic scattering experiment suggests that the  $2_1^+$  state of  $^{16}\text{C}$  is formed nearly by valence

neutron excitations [4]. Finally  $\alpha$ -cluster configurations appear to play no active role in  $^{15,16}\text{C}$ , so excitations of the  $^{14}\text{C}$  core can be neglected as a first trial. Note that in  $^{16}\text{C}$  the  $^{12}\text{Be}+\alpha$  threshold is 13.81 MeV, much higher than that of  $^{14}\text{C}+2n$  (5.47 MeV).

At the same time we will analyze the  $B(E2)$  values of the normal nuclei  $^{17,18}\text{O}$  and  $^{17}\text{F}$ ,  $^{18}\text{Ne}$ . For these nuclei, however, we anticipate that the  $^{16}\text{O}$  core plus valence-nucleon model is not as good as for  $^{15,16}\text{C}$ . For example, the  $\alpha$  threshold of  $^{17}\text{O}$  is just 2.22 MeV above the  $^{16}\text{O}+n$  threshold, and in  $^{18}\text{O}$  the  $\alpha$  threshold becomes lowest (6.23 MeV), much lower than the  $^{16}\text{O}+2n$  threshold (12.19 MeV). See Refs. [10–13] for the importance of the  $\alpha$  correlation or multi-particle-hole excitations in  $^{18}\text{O}$ . In the case of  $^{17}\text{F}$  and  $^{18}\text{Ne}$  the  $\alpha$  threshold is still low though higher than the  $^{16}\text{O}+p$  or  $^{16}\text{O}+2p$  threshold.

It is instructive to rewrite the  $E2$  operator according to our model. Suppose that the core has mass number  $A_c$  and atomic number  $Z_c$  while the valence-nucleon part mass number  $A_v$  and atomic number  $Z_v$  ( $A=A_c+A_v$ ). The  $E2$  operator  $\mathcal{M}_\mu(A)=e\sum_{i=1}^A e_i \mathcal{Y}_{2\mu}(\mathbf{r}_i-\mathbf{X}_A)$ , where  $e_i$  is the charge of the  $i$ th nucleon (in units of  $e$ ),  $\mathbf{X}_A$  the center-of-mass coordinate of the system, and  $\mathcal{Y}_{lm}(\mathbf{r})=r^l Y_{lm}(\hat{\mathbf{r}})$  can be expressed as

$$\mathcal{M}_\mu(A) = \mathcal{M}_\mu(c) + \mathcal{M}_\mu(v) + qe\mathcal{Y}_{2\mu}(\mathbf{R}) + \cdots, \quad (1)$$

$$q = \left(\frac{A_v}{A}\right)^2 \sum_{i \in \text{core}} e_i + \left(\frac{A_c}{A}\right)^2 \sum_{i \in \text{valence}} e_i = \left(\frac{A_v}{A}\right)^2 Z_c + \left(\frac{A_c}{A}\right)^2 Z_v, \quad (2)$$

where  $\mathbf{R}=\mathbf{X}_c-\mathbf{X}_v$  is the relative distance vector from the core's center-of-mass to that of the valence nucleons and the ellipsis denotes those parts which couple the electric dipole operator of the core with the dipole operator for the relative motion and the analogous one for the valence-nucleon part. The first and second terms on the right-hand side of Eq. (1) stand for the  $E2$  operators for the core and valence parts, respectively, and the third term the  $E2$  operator for the relative motion between them.

The utility of the above formula is exemplified by an extreme case that the valence nucleons form a cluster with  $J=0$ . In this case the  $E2$  operator  $\mathcal{M}_\mu(v)$  for the valence part makes no contribution. A good example to apply the cluster model is the  $B(E2)$  transition in  $^{16}\text{O}$  from the  $2^+$  state at 6.92 MeV to the  $0^+$  state at 6.05 MeV because these states are well described with an  $\alpha$ -cluster orbiting around the  $^{12}\text{C}$  core [14]. The  $B(E2)$  value is calculated through a radial matrix element  $I = \int_0^\infty u_0(R)u_2(R)R^4 dR$ , where  $u_0(R)$  and  $u_2(R)$  are the relative motion functions with  $L=0$  and 2. We generated them from a potential  $-102.46 e^{-0.12R^2}$  (MeV) together with the Coulomb potential, which reproduces the binding energies of the two states with appropriate node numbers. The resulting  $B(E2)$  value is  $52 e^2 \text{fm}^4$ , in fair agreement with experiment,  $65 \pm 7 e^2 \text{fm}^4$  [15].

We used the bare charge for the nucleon to arrive at Eq. (2). The effect of the distortion or polarization of the core is renormalized as an effective charge. By assuming that the polarization charge  $\delta$  is isoscalar, the charge  $q$  of the third term in Eq. (1) is subject to a change

$$q \rightarrow q_{\text{eff}} = q + \left(\frac{A_c}{A}\right)^2 A_v \delta. \quad (3)$$

It is important to note that, when the valence nucleons are all neutrons ( $Z_v=0$ ) and  $A_v$  is much smaller than  $A$ ,  $q^2$  becomes very small but  $q_{\text{eff}}^2$  may become fairly large. For instance, in the case of  $^{16}\text{C} = ^{14}\text{C} + 2n$   $q^2$  is only 0.0088 but increases drastically to  $q_{\text{eff}}^2=0.16$  for  $\delta=0.2$ , a typical value used in shell-model calculations. However, when the valence part contains at least one proton,  $q^2$  is already large and the change of  $q^2$  to  $q_{\text{eff}}^2$  is rather moderate. For  $^{17}\text{F} = ^{16}\text{O} + p$   $q^2$  is 0.83 and changes to  $q_{\text{eff}}^2=1.19$  for  $\delta=0.2$ .

The wave function for two like nucleons is determined from the following Hamiltonian:

$$H = T_R + T_r + U_1 + U_2 + v_{12}, \quad (4)$$

where  $\mathbf{r}$  is the relative distance vector of the valence nucleons.  $U_i$  is the nucleon-core potential, and  $v_{12}$  is the potential between the valence nucleons. The Coulomb potential is taken into account. As  $U$  we use

$$U = -V_0 f(r) + V_1 \ell \cdot s \frac{1}{r} \frac{d}{dr} f(r) + V_{\text{Coul}}, \quad (5)$$

where  $f(r) = \{1 + \exp[(r - R_c)/a]\}^{-1}$  with  $R_c = r_0 A_c^{1/3}$  and we set  $a = 0.65$  fm and  $r_0 = 1.25$  fm. Other parameters of  $U$  are determined to reproduce the single-particle energies of the nucleon+core system:  $V_0$  are 50.31, 52.98, 53.20 MeV and  $V_1$  are 16.64, 23.23, 22.13 MeV fm<sup>2</sup>, for  $n + ^{14}\text{C}$ ,  $p + ^{16}\text{O}$ ,  $n + ^{16}\text{O}$ , respectively. For  $v_{12}$  we take the singlet-even part of the Minnesota potential [16]:  $200e^{-1.487r^2} - 91.85\gamma e^{-0.465r^2}$  (MeV), where  $\gamma$  is unity for the Minnesota potential but adjusted to reproduce the ground-state energy of the core+two-nucleon system. We assume that two like nucleons are in the spin-singlet state. The spin-orbit potential in Eq. (5) thus makes no contribution to the energy. Trial wave functions for the ground ( $0^+$ ) and excited ( $2^+$ ) states are

expressed in terms of a combination of correlated Gaussians,  $\Psi_{LM}(1,2) = \sum_{i=1}^K C_i \Psi_{LM}(A_i, \mathbf{v}_i)$  ( $L=0,2$ ):

$$\Psi_{LM}(A, \mathbf{v}) = (1 - P_{12}) \{e^{-1/2\tilde{\mathbf{x}}A\tilde{\mathbf{x}}} \mathcal{Y}_{LM}(\mathbf{v}) \chi_{S=0}(1,2)\}, \quad (6)$$

where the permutation  $P_{12}$  assures the antisymmetry requirement,  $\tilde{\mathbf{x}}A\tilde{\mathbf{x}}$  is a short-hand notation for  $A_{11}\mathbf{x}_1^2 + 2A_{12}\mathbf{x}_1 \cdot \mathbf{x}_2 + A_{22}\mathbf{x}_2^2$ , and a global vector,  $\mathbf{v} = u_1\mathbf{x}_1 + u_2\mathbf{x}_2$ , specified by  $(u_1, u_2)$ , describes the rotational motion of the system [17,18]. The coordinates  $\mathbf{x}_1$  and  $\mathbf{x}_2$  are the distance vectors of the nucleons from the core's center-of-mass  $\mathbf{x}_1 = \mathbf{R} + \frac{1}{2}\mathbf{r}$ ,  $\mathbf{x}_2 = \mathbf{R} - \frac{1}{2}\mathbf{r}$ . The two nucleons are explicitly correlated as the correlated Gaussian contains a cross term  $A_{12}\mathbf{x}_1 \cdot \mathbf{x}_2$  in the exponent. The inclusion of this term is quite different from the previous cluster-orbital shell-model calculations [19], which led to slow convergence due to the absence of such cross terms.

It is vital to take into account the Pauli principle for the motion of the valence nucleons. This is done by requiring that the trial wave function has no overlap with all the orbits  $u_{nljm}$  occupied in the core

$$\langle u_{nljm}(i) | \Psi_{LM}(1,2) \rangle = 0 \quad (i=1,2), \quad (7)$$

where the single-particle orbit  $u_{nljm}$  is generated from  $U$  and  $nlj$  runs over  $0s_{1/2}$ ,  $0p_{3/2}$ ,  $0p_{1/2}$  for  $^{16}\text{C}$ . The coordinates  $\mathbf{x}_1$  and  $\mathbf{x}_2$  are most convenient to satisfy Eq. (7) as the spatial part of  $u_{nljm}(i)$  is a function of  $\mathbf{x}_i$ . The requirement (7) is practically achieved by the orthogonal projection method [20]. The probability of mixing-in of the occupied orbits was actually small, typically  $10^{-4}$ . See, e.g., Ref. [21] for other way to treat three-body systems with Pauli principle and core excitation.

An upper bound for the energy is given by the eigenvalue of the generalized eigenvalue problem

$$\sum_{j=1}^K H_{ij} C_j = E \sum_{j=1}^K B_{ij} C_j \quad (i=1,2, \dots, K), \quad (8)$$

$$\begin{pmatrix} H_{ij} \\ B_{ij} \end{pmatrix} = \langle \Psi_{LM}(A_i, \mathbf{v}_i) | \begin{pmatrix} H \\ 1 \end{pmatrix} | \Psi_{LM}(A_j, \mathbf{v}_j) \rangle. \quad (9)$$

The matrix elements are evaluated by the method given in Ref. [18]. Each basis function is specified by four parameters ( $A_{11}, A_{12}, A_{22}, u_1$ ), as  $u_1^2 + u_2^2$  can be chosen arbitrary, say unity.  $u_1$  is redundant for  $L=0$ . The energy (the wave function as well) is a function of 4K (or 3K) nonlinear parameters, and crucially depends on the choice of these parameters. We used the algorithm called the stochastic variational method (SVM) [18] to optimize the parameters. The SVM increases the basis dimension one by one by testing a number of candidates which are chosen randomly and in addition fine-tunes the already chosen parameters by a refinement process. Many examples have shown that this procedure is powerful to set up such a basis set that gives a virtually exact solution.

Figure 1 displays the energies of  $^{16}\text{C}$  as a function of basis dimension. The value of  $\gamma$  was 1.20. Also shown are those energies which are obtained in the noncorrelated Gaussians ( $A_{12}=0$ ). The noncorrelated basis misses the energy by about

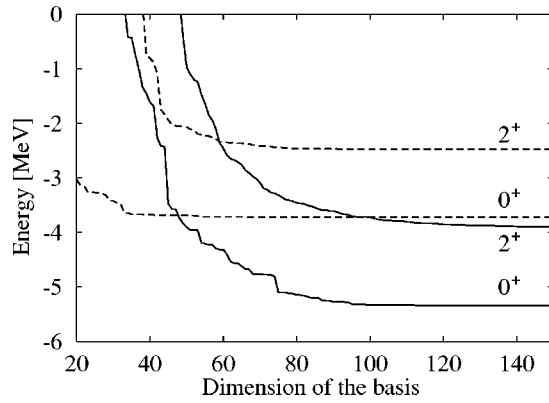


FIG. 1. Energies, from the  $^{14}\text{C}+2n$  threshold, of the ground and first excited states of  $^{16}\text{C}$  as a function of basis dimension. Solid and dashed lines denote the results with the correlated and noncorrelated basis calculations, respectively.

1.6 MeV compared to the correlated basis calculation. Table I lists the results of calculation. The spacing between the ground and  $2^+$  excited states is in fair agreement with experiment. The  $0_2^+$  state is predicted at the excitation energy of 2.94 MeV, which is also close to experiment. The mean square radius of the nucleon distribution for  $^{15,16}\text{C}$  is related to that of  $^{14}\text{C}$ :  $r^2(^{15}\text{C}) = \frac{14}{15}r^2(^{14}\text{C}) + \frac{14}{225}\langle x_1^2 \rangle$  and  $r^2(^{16}\text{C}) = \frac{14}{16}r^2(^{14}\text{C}) + \frac{7}{64}\langle R^2 \rangle + \frac{8}{256}\langle r^2 \rangle$ . Note that  $\langle x_2^2 \rangle = \langle x_1^2 \rangle$ . The mean square radius  $r^2(^{14}\text{C})$  is not known but expected to be slightly larger than the point-proton radius  $(2.35 \text{ fm})^2$  [22]. Thus the mean square radius of  $^{15}\text{C}$  is concluded to be larger than that of  $^{16}\text{C}$ .

The probability of finding the spin-singlet neutrons in the  $1s_{1/2}$  or  $0d_{5/2}$  radial function of  $^{15}\text{C}$  is calculated. For the ground state of  $^{16}\text{C}$ , the  $(1s_{1/2})^2$  probability is 0.49 and the  $(0d_{5/2})^2$  probability is 0.39. The missing probability (0.13) signals the importance of unbound single-particle orbits or continuum states of  $^{15}\text{C}$ . The two probabilities scaled to add up to unity are similar to the shell-model result with LSF matrix elements [9]. For the  $0_2^+$  state the  $(1s_{1/2})^2$  and  $(0d_{5/2})^2$  probabilities are 0.47 and 0.49, respectively. For the  $2^+$  state the  $1s_{1/2}0d_{5/2}$  probability is largest (0.68).

The  $B(E2)$  value for the  $2^+ \rightarrow 0^+$  transition in  $^{16}\text{C}$  was calculated according to the decomposition (1). Figure 2 displays the  $B(E2)$  values of  $^{15,16}\text{C}$  as a function of the polarization charge  $\delta$ . With  $\delta=0$  the calculation gives too small values to compare with experiment. To reproduce the data we need  $\delta \approx 0.16$  for  $^{15}\text{C}$  and  $\delta = 0.098 \pm 0.012$  for  $^{16}\text{C}$ . If we

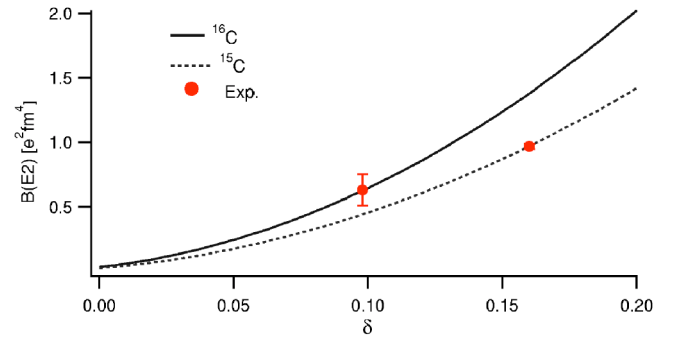


FIG. 2. (Color online) The  $B(E2)$  values for transitions from the first excited state to the ground state in  $^{15,16}\text{C}$  as a function of the polarization charge  $\delta$ . Data for  $^{16}\text{C}$  are taken from Refs. [3,4].

use the same  $\delta$  as  $^{15}\text{C}$  the  $B(E2)$  of  $^{16}\text{C}$  becomes about twice larger than experiment. The polarization charges needed to fit the data are not very large, which supports the present model. The difference of the charges required for  $^{15}\text{C}$  and  $^{16}\text{C}$  is much smaller than the other cases as will be shown in Table II. The hindered  $B(E2)$  value of  $^{16}\text{C}$  can be reproduced naturally without invoking any unusual assumptions. The third term of Eq. (1) contributes to the  $B(E2)$  value about two times more than the  $\mathcal{M}_\mu(\nu)$  term, and their cross term accounts for about a half of the  $B(E2)$  value.

Table II summarizes the  $E2$  transition probabilities. The  $\gamma$  value was chosen as 1.28 for  $^{18}\text{Ne}$  and 1.27 for  $^{18}\text{O}$ . The  $B(E2)$  of  $^{17}\text{F}$  can be reproduced with a small  $\delta$  (0.095), but the transition in  $^{18}\text{Ne}$  requires a much larger value ( $\delta = 0.29$ ). This clearly indicates that the relevant states in  $^{18}\text{Ne}$  are not well described with the simple  $^{16}\text{O}+2p$  model but contain core excited configurations such as  $4p-2h$  or  $\alpha + ^{14}\text{O}$ . Similarly the fact that the  $\delta$  needed for  $^{17}\text{O}$  is as large as 0.40 suggests that the low-lying states of  $^{17}\text{O}$  contain much of  $\alpha$ -cluster configurations as noted in the beginning. The  $\delta$  needed for the transition in  $^{18}\text{O}$  is even larger (0.61), which again indicates significant amount of such core excited configurations as described with the  $\alpha + ^{14}\text{C}$  model [10].

The quality of the wave functions obtained for  $^{15,16}\text{C}$  can be tested by the longitudinal momentum distribution of  $^{15}\text{C}$  fragment from the breakup of  $^{16}\text{C}$  [6,7]. The reaction dynamics can be incorporated in the Glauber or eikonal approximation [24,25]. We calculated the momentum distribution due to the inelastic breakup process by using the following formula [24]:

TABLE I. Properties of the ground and excited states in  $^{15,16}\text{C}$ .  $E$  is the energy from the  $^{14}\text{C}+n$  or  $^{14}\text{C}+2n$  threshold. Energy and length are in MeV and fm, respectively.

Nucleus	State	$E_{\text{cal}}$	$E_{\text{exp}}$	$\langle x_1^2 \rangle$	$\langle R^2 \rangle$	$\langle r^2 \rangle$	$\langle x_1 \cdot x_2 \rangle$
$^{15}\text{C}$	$\frac{1}{2}^+$	-1.218	-1.218	30.37			
	$\frac{5}{2}^+$	-0.478	-0.478	17.50			
$^{16}\text{C}$	$0_1^+$	-5.34	-5.469	16.81	9.43	29.52	2.05
	$2_1^+$	-3.90	-3.699	15.35	8.27	28.30	1.19
	$0_2^+$	-2.39	-2.466	21.31	11.21	40.40	1.11

TABLE II.  $B(E2)$  transition probabilities in units of  $e^2 \text{fm}^4$ .  $B(E2)_{\text{cal}}$  is obtained with no polarization charge.  $\delta_{\text{exp}}$  is the polarization charge needed to reproduce experiment.

Nucleus	Initial	Final	$B(E2)_{\text{exp}}$	$B(E2)_{\text{cal}}$	$\delta_{\text{exp}}$
$^{15}\text{C}$	$\frac{5}{2}^+$	$\frac{1}{2}^+$	$0.97 \pm 0.02^{\text{a}}$	0.025	0.16
$^{16}\text{C}$	$2^+$	$0^+$	$0.63 \pm 0.12^{\text{b}}$	0.034	0.098
$^{17}\text{F}$	$\frac{1}{2}^+$	$\frac{5}{2}^+$	$64.9 \pm 1.3^{\text{c}}$	55.4	0.095
$^{18}\text{Ne}$	$2^+$	$0^+$	$49.6 \pm 5.0^{\text{d}}$	30.0	0.29
$^{17}\text{O}$	$\frac{1}{2}^+$	$\frac{5}{2}^+$	$6.21 \pm 0.08^{\text{c}}$	0.032	0.40
$^{18}\text{O}$	$2^+$	$0^+$	$9.30 \pm 0.25^{\text{d}}$	0.026	0.61

<sup>a</sup>Ref. [22].

<sup>b</sup>Ref. [3,4].

<sup>c</sup>Ref. [15].

<sup>d</sup>Ref. [23].

$$\begin{aligned} \frac{d\sigma_{-n}}{dP_{\parallel}} &= \frac{1}{2\pi\hbar} \int db_n (1 - e^{-2 \text{Im} \chi_{nT}(b_n)}) \\ &\times \int ds e^{-2 \text{Im} \chi_{FT}(b_n-s)} \frac{1}{2l+1} \\ &\times \sum_{m=-l}^l \left| \int dz e^{(i/\hbar)P_{\parallel}z} g_{lj}(r) Y_{lm}(\hat{r}) \right|^2, \quad (10) \end{aligned}$$

where  $g_{lj}(r)$  is the radial part of the spectroscopic amplitude  $\langle \Psi_{ljm}(^{15}\text{C}) | \Psi_{00}(^{16}\text{C}) \rangle$ . The distribution is contributed by the breakup of  $^{16}\text{C}$  to the  $\frac{1}{2}^+$  and  $\frac{5}{2}^+$  states of  $^{15}\text{C}$ . As is clear, the distribution basically probes the Fourier transform of the wave function  $g_{lj}(r)$  of the last neutron in  $^{16}\text{C}$ . We used the nucleon-target ( $^{12}\text{C}$ ) global optical potential [26] to calculate the nucleon-target ( $\chi_{nT}$ ) and  $^{15}\text{C}$  fragment-target ( $\chi_{FT}$ ) phase shift functions. Details of calculation will be published elsewhere. Figure 3 compares the theory with experiment. Relative contributions of both the  $\frac{1}{2}^+$  and  $\frac{5}{2}^+$   $^{15}\text{C}$  fragments are naturally determined by the wave functions of  $^{15,16}\text{C}$ . It is seen that they contribute to the distribution quite differently.

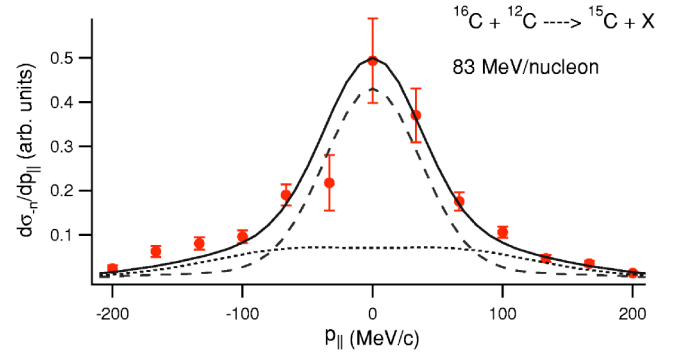


FIG. 3. (Color online) The distribution of  $^{15}\text{C}$  fragments from  $^{16}\text{C}$  breakup at 83 MeV/nucleon as a function of the longitudinal momentum  $p_{\parallel}$ . The contributions of the  $\frac{1}{2}^+$  and  $\frac{5}{2}^+$  fragments of  $^{15}\text{C}$  are shown by dashed and dotted lines, respectively. Data are taken from Ref. [6].

The  $s$  orbit is spatially more extended than the  $d$  orbit, so that it produces a narrower momentum distribution. As the experiment is well reproduced, the wave function of  $^{16}\text{C}$  can be judged acceptable.

To conclude, we have studied the anomaly of the  $E2$  transition in  $^{16}\text{C}$  in the  $^{14}\text{C}+n+n$  model. It turns out that the model is reasonable to account for the hindered transition strength as well as the longitudinal momentum distribution of  $^{15}\text{C}$  fragments from  $^{16}\text{C}$  breakup. The soundness of the model is confirmed by studying the  $B(E2)$  values in ( $^{17}\text{O}$ ,  $^{18}\text{O}$ ) and ( $^{17}\text{F}$ ,  $^{18}\text{Ne}$ ) nuclei, where considerably different polarization charges are needed to fit the  $A=18$ , 18, pair compared to the  $^{15,16}\text{C}$  case. An open question is, however, why the polarization charge for  $^{16}\text{C}$  is smaller than that of  $^{15}\text{C}$ . A more sophisticated calculation will be called for which includes other effects such as spin-triplet component, noncentral forces, and core excitations.

One of the authors (B. A-I.) was supported by the JSPS for foreign researchers (Grant No. P03023). This work was in part supported by JSPS Grants-in-Aid for Scientific Research (Grant Nos. 14540249 and 15-03023).

[1] T. Motobayashi *et al.*, Phys. Lett. B **346**, 9 (1995).  
 [2] H. Scheit *et al.*, Phys. Rev. Lett. **77**, 3967 (1996).  
 [3] N. Imai *et al.*, Phys. Rev. Lett. **92**, 062501 (2004).  
 [4] Z. Elekes *et al.*, Phys. Lett. B **586**, 34 (2004).  
 [5] D. Q. Fang *et al.*, Phys. Rev. C **69**, 034613 (2004).  
 [6] T. Yamaguchi *et al.*, Nucl. Phys. **A724**, 3 (2003).  
 [7] V. Maddalena *et al.*, Phys. Rev. C **63**, 024613 (2001).  
 [8] H. G. Bohlen *et al.*, Phys. Rev. C **68**, 054606 (2003).  
 [9] H. T. Fortune *et al.*, Phys. Rev. Lett. **40**, 1236 (1978).  
 [10] T. Sakuda, Prog. Theor. Phys. **57**, 855 (1977).  
 [11] Y. Suzuki, A. Yamamoto, and K. Ikeda, Nucl. Phys. **A444**, 365 (1985).  
 [12] H. T. Fortune and S. C. Headley, Phys. Lett. **51B**, 136 (1974).  
 [13] R. L. Lawson, F. J. D. Serduke, and H. T. Fortune, Phys. Rev. C **14**, 1245 (1976).

[14] Y. Suzuki, Prog. Theor. Phys. **55**, 1751 (1976); **56**, 111 (1976).  
 [15] D. R. Tilley, H. R. Weller, and C. M. Cheves, Nucl. Phys. **A564**, 1 (1993).  
 [16] R. Thompson, M. Lemere, and Y. C. Tang, Nucl. Phys. **A286**, 53 (1977).  
 [17] Y. Suzuki, J. Usukura, and K. Varga, J. Phys. B **31**, 31 (1998).  
 [18] Y. Suzuki and K. Varga, *Stochastic Variational Approach to Quantum-Mechanical Few-Body Problems, Vol. 54 of Lecture Notes in Physics* (Springer, Berlin, 1998); K. Varga and Y. Suzuki, Phys. Rev. C **52**, 2885 (1995).  
 [19] Y. Suzuki and K. Ikeda, Phys. Rev. C **38**, 410 (1988); Y. Tosaka and Y. Suzuki, Nucl. Phys. **A512**, 46 (1990).  
 [20] V. I. Kukulin and V. N. Pomerantsev, Ann. Phys. (N.Y.) **111**, 330 (1978).

- [21] F. M. Nunes, J. A. Christley, I. J. Thompson, R. C. Johnson, and V. D. Efros, Nucl. Phys. **A609**, 43 (1996); F. M. Nunes, I. J. Thompson, and J. A. Tostevin, *ibid.* **A703**, 593 (2002).
- [22] F. Azjenberg-Selove, Nucl. Phys. **A523**, 1 (1991).
- [23] D. R. Tilley, H. R. Weller, C. M. Cheves, and R. M. Chasteler, Nucl. Phys. **A595**, 1 (1995).
- [24] B. Abu-Ibrahim, Y. Ogawa, Y. Suzuki, and I. Tanihata, Comput. Phys. Commun. **151**, 369 (2003).
- [25] K. Hencken, G. F. Bertsch, and H. Esbensen, Phys. Rev. C **54**, 3043 (1996).
- [26] E. D. Cooper, S. Hama, B. C. Clark, and R. L. Mercer, Phys. Rev. C **47**, 297 (1993).